

Effects of the Magnetic Fields on Ion Beam Energy in a Magnetically Expanding Plasma

Kazunori TAKAHASHI, Yutaka SHIDA and Tamiya FUJIWARA

Department of Electrical and Electronic Engineering, Iwate University, Morioka 020-8551, Japan

(Received: 22 October 2009 / Accepted: 29 January 2010)

Effects of the magnetic-field configuration on electrostatic ion acceleration in a magnetically expanding plasma source are experimentally investigated, where an expanding plasma machine with two solenoid coils is manufactured. The field configurations can be changed by adjusting the solenoid currents. The 13.56 MHz radiofrequency power for plasma production and the argon gas pressure are maintained at 250 W and 80 mPa, respectively. The ion energy distribution functions near the source exit show the existence of the accelerated group of ions and demonstrate that the ion beam energy has a maximum for the magnetic fields uniform axially inside the source tube. The results would play an important role in the optimization of the recently-developed expanding plasma source using permanent magnets, which can generate the supersonic ion beam due to a formation of an electric double layer.

Keywords: expanding plasmas, diverging magnetic fields, electrostatic ion acceleration, double layer, ion energy distribution function

1. Introduction

Magnetically expanding radiofrequency plasmas containing an electric double layer (DL) have recently been vigorous and interesting research subject in connection with the development of electrodeless electric propulsion devices [1, 2] and with the particle acceleration physics in space plasmas [3, 4]. Due to the formation of the DL in the magnetically expanding plasmas, electrostatically and supersonically accelerated beam of ions have been detected in various experimental machines by retarding field energy analyzers (RFEAs) [1, 5, 6] and laser induced fluorescence methods [7, 8, 9]. In the series of the studies on the magnetically expanding plasmas, it is reported in the experiments [10, 11, 12] and in the particle-in-cell simulations [13] that only the single plasma source upstream of the DL is required for maintaining the DL and the subsequent generation of the ion beam, where energetic electrons upstream of the DL can overcome the potential drop of the DL and neutralize the ion beam. Therefore, the above-mentioned mechanism of the ion acceleration can be utilized for the development of the electrodeless and neutralizer-free propulsion device, called helicon double layer thruster [14].

In the previously reported helicon-plasma systems containing the DL, the electromagnets have been used to create the expanding magnetic-field configurations. The use of the electromagnets would yield flexibility on control of the magnetic-field configurations, whereas it would increase the consumed electric power and make the system large. The authors have already

reported the new type of the magnetically-expanding, compact plasma source with a diverging magnetic-field configuration provided by only permanent magnets (PMs) instead of the electromagnets, where a 6.5-



Fig. 1 (Color online) (a) Photograph of the presently-manufactured magnetically-expanding plasma device using electromagnets with 6.5-cm-diameter source tube.

author's e-mail: kazunori@iwate-u.ac.jp

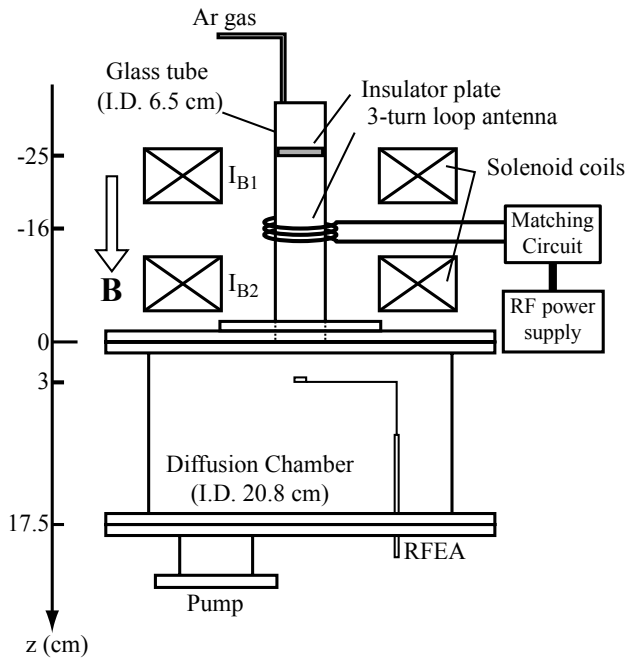


Fig. 2 Schematic diagram of the magnetically-expanding plasma device using electromagnets with 6.5-cm-diameter source tube.

cm-diameter source tube has been set up [6, 15, 16]. In the aforementioned experiments on the PMs compact source, the formation of the DL structure and the subsequent generation of the supersonic ion beam with energy corresponding to the potential drop of the DL are simultaneously observed by the RFEAs, where the potential drop of the DL and the ion beam energy appear to be larger than the expanding plasma source using the electromagnets [17]. Since the thrust force of the plasma thruster utilizing the electrostatic ion acceleration, called an ion engine, is proportional to the square root of the ion beam energy, the higher energy of the ion beam is useful for the application to the propulsion devices. The optimization of the expanding plasma source using the PMs, especially, the improvement of the magnetic-field configuration, is required now, but it is not easy to perform the experiments for various magnetic-field configurations in the PMs expanding plasma machine because of their inflexibility.

In order to optimize the magnetic-field configuration in the PMs compact source with the 6.5-cm-diameter source tube, it is important to know the behavior of the ion acceleration for various magnetic-field configurations at first. The effect of the magnetic-field configurations have been experimentally investigated in the expanding plasma system with 14-cm-diameter source tube and two solenoid coils [18, 19]. However, it is doubtful whether the comparison between our PMs expanding plasma machine and the 14-cm-diameter expanding plasma machine is reli-

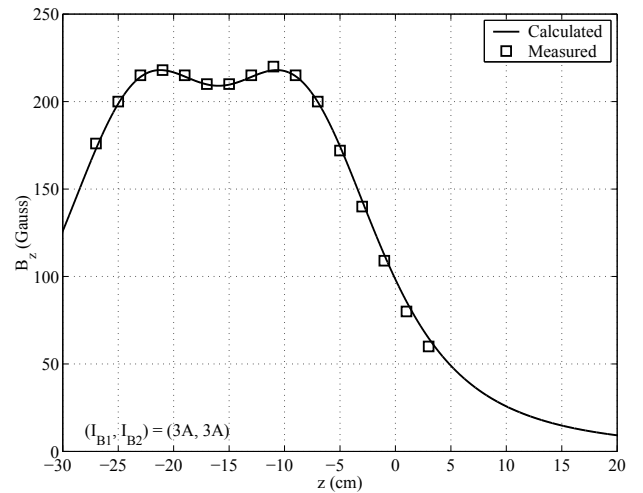


Fig. 3 The measured (open squares) and calculated (solid line) axial profiles of the axial component B_z of the magnetic-field strength for $(I_{B1}, I_{B2}) = (3 \text{ A}, 3 \text{ A})$.

able or not. Hence, we now manufacture a new magnetically-expanding plasma device with a 6.5-cm-diameter source tube and with two solenoid coils, shown in Fig. 1. In the present paper, the characteristics of the ion beam detected near the source exit for various magnetic-field configurations are reported, where the field configuration can be changed by adjusting the two solenoid currents. The results reported here would be fed back to the optimized design of the PMs compact source in the near future. In Sec. 2, the experimental setup of the recently manufactured machine is described, and the results are shown in Sec. 3. Based on the results on the expanding plasma machine with the 6.5-cm-diameter source tube and the solenoid coils, the design of the PMs expanding plasma source is discussed in Sec. 4. Conclusions are given in Sec. 5.

2. Experimental Setup

Figures 1 and 2 show the photograph and the schematic diagram of the presently-manufactured magnetically-expanding plasma device using electromagnets with the 6.5-cm-inner-diameter source tube, respectively. The machine has a 35-cm-long and 6.5-cm-diameter cylindrical glass tube (source tube) and a 17.5-cm-long and 20.8-cm-diameter stainless steel vacuum chamber (diffusion chamber). The interfaces between the source tube and the diffusion chamber, and between the source tube and the upstream flange are sealed using O-rings; then the chamber is evacuated to a base pressure below 1 mPa by a rotary/diffusion pumping system connected to the downstream side of the diffusion chamber through a NW-40 vacuum port. The interface between the source tube and the diffusion chamber, i.e., the source exit, is defined as $z = 0$, where z is the axial position as shown in Fig. 2. The

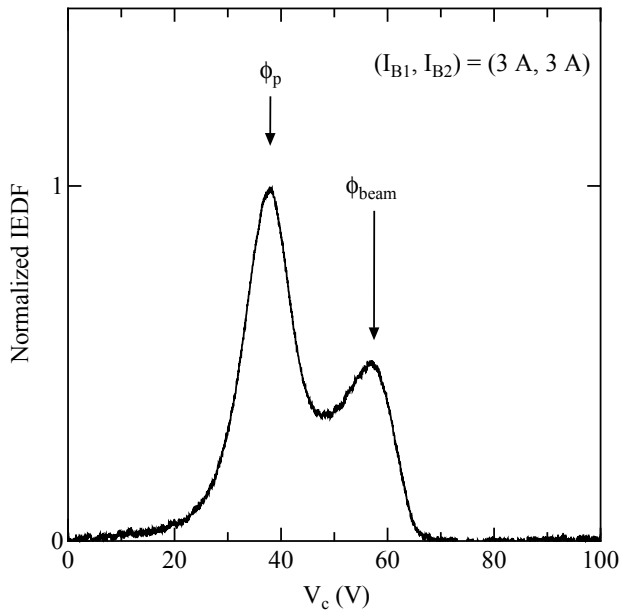


Fig. 4 The measured IEDF at $z = 3$ cm downstream of the source exit for $(I_{B1}, I_{B2}) = (3 \text{ A}, 3 \text{ A})$.

pressure in the vacuum chamber is measured by an ionization gauge connected to a sideport of the diffusion chamber. The argon gas is introduced from the source side through 1/4-inch stainless steel pipe connected to the upstream flange, where the flow rate of the argon gas and the gas pressure in the vacuum chamber is maintained at a few sccm and 80 mPa by a mass flow controller with maximum flow rate of 10 sccm. A 13.56 MHz radiofrequency generator supplies 200 W power to the triple-turn rf loop antenna winding the 7-cm-outer-diameter source tube at $z = -16$ cm; then the argon plasma is produced by an inductively coupled discharge.

Two solenoid coils are situated at $z = -8.7$ cm and $z = -23.2$ cm, and the magnetic-field configurations can be changed by adjusting the two currents fed to these coils. The currents fed to the upstream ($z = -23.2$ cm) and the exhaust ($z = -8.7$ cm) coils are labeled as I_{B1} and I_{B2} , respectively, which can be changed in the range of 0-5 A. Figure 3 shows the measured (open squares) and calculated (solid line) axial profiles of the axial component B_z of the magnetic-field strength for $(I_{B1}, I_{B2}) = (3 \text{ A}, 3 \text{ A})$, where the B_z is measured by a gaussmeter and calculated from the Biot-Savart law. It is found that the measured B_z agree well with the calculated result and show about 210 G at the middle of the two coils at $z = -16$ cm; we can estimate the magnetic-field configuration from the calculated results for various coil currents hereafter.

An ion energy distribution function (IEDF) is measured by a retarding field energy analyzer (RFEA) with an entrance orifice facing the source tube and located at $z = 3$ cm near the source exit, which is in-

serted from the downstream port with vacuum seal. The RFEA consists of an electron reflector mesh biased at -60 V, an ion collector electrode, and a 3-mm-diameter entrance orifice, where the IEDF is also measured by the multi-mesh RFEA [20] then the results have not been changed. The IEDF is proportional to the first derivative (dI_c/dV_c) of I_c - V_c curve, where I_c and V_c are the collector current and the collector voltage, respectively. The measurement of the first derivative, i.e., the IEDF, is performed by a pulsed probe technique resembling the measurement of the electron energy probability functions [21, 10]; the details of which will be described in our recent paper [22]. Briefly, when the collector voltage V_c is swept linearly during about 25 ms time, the current I_c signal converted into voltage signal through 10 k Ω resistor is differentiated using an active analog circuit, which acts as a differentiator for I_c - V_c trace and as a rejecting filter for plasma instabilities and electric noise above about 1 kHz. The signals of I_c and V_c are digitized by a digital storage oscilloscope (Tektronix TDS2024), and passed into a LABVIEW program through a GPIB interface for conversion into an ASCII data file and display on a computer.

3. Experimental Results

Figure 4 shows the IEDF measured by the axially facing RFEA at $z = 3$ cm for $(I_{B1}, I_{B2}) = (3 \text{ A}, 3 \text{ A})$, i.e., for the magnetic-field configuration shown in Fig. 3. The IEDF clearly has two peaks at $V_c \sim 38$ V and $V_c \sim 57$ V; it implies the existence of the accelerated group of ions at $V_c \sim 57$ V in addition to the bulk ions at $V_c \sim 38$ V. The left- and right-side peaks give us the information on the local plasma potential ϕ_p and the beam potential ϕ_{beam} as indicated by solid arrows in Fig. 4, where note that the beam “potential” is different from the beam “energy”. Since the zero energy of the ions are corresponding to the local plasma potential ϕ_p according to the principle of the RFEA measurement, the energy ε_{beam} of the accelerated beam of ions can be derived as $\varepsilon_{beam} \equiv \phi_{beam} - \phi_p$. Hence, the energy of the ion beam observed in Fig. 4 can be estimated as about 19 eV. The velocity v_{beam} of the beam ions with energy ε_{beam} is derived as

$$v_{beam} = \sqrt{\frac{2e\varepsilon_{beam}}{M_i}}, \quad (1)$$

where M_i and e are the ion mass and the elementary charge, respectively. The ion beam velocity for $\varepsilon_{beam} = 19$ eV is 9.5 km/s. As the ion sound speed C_s calculated for the measured electron temperature ($T_e \sim 8$ eV) is 4.4 km/s, the observed ion beam is found to be supersonic. The Mach number M of the ion beam is estimated as $M \sim 2.2$. The above-

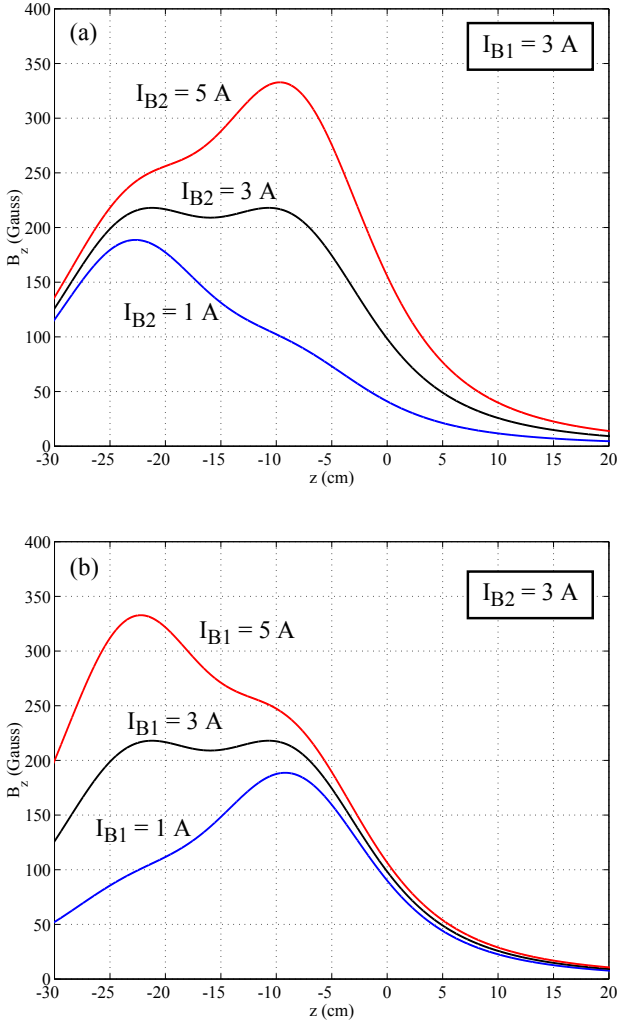


Fig. 5 (Color online) Axial profiles of the calculated magnetic-field strength B_z (a) as a function of I_{B2} for $I_{B1} = 3$ A, and (b) as a function of I_{B1} for $I_{B2} = 3$ A.

mentioned result is very similar to that in the previously reported 14-cm-diameter expanding plasma experiments [23].

The measurement of the IEDF is performed for various magnetic-field configuration. The magnetic-field configurations are changed by adjusting the exhaust-coil current I_{B2} under the constant upstream-coil current ($I_{B1} = 3$ A), or by adjusting the I_{B1} under the constant exhaust-coil current ($I_{B2} = 3$ A). Figures 5(a) and 5(b) show the axial profiles of the calculated magnetic-field strength B_z as a function of I_{B2} for $I_{B1} = 3$ A, and as a function of I_{B1} for $I_{B2} = 3$ A, respectively. The axial profile of B_z is found to be uniform when the equal currents are fed to the two solenoid coils, i.e., $(I_{B1}, I_{B2}) = (3$ A, 3 A). It is found that the magnetic-field configuration in the source tube can be changed into uniform, divergent, and convergent by the coil currents with keeping the expanding field lines near the source exit.

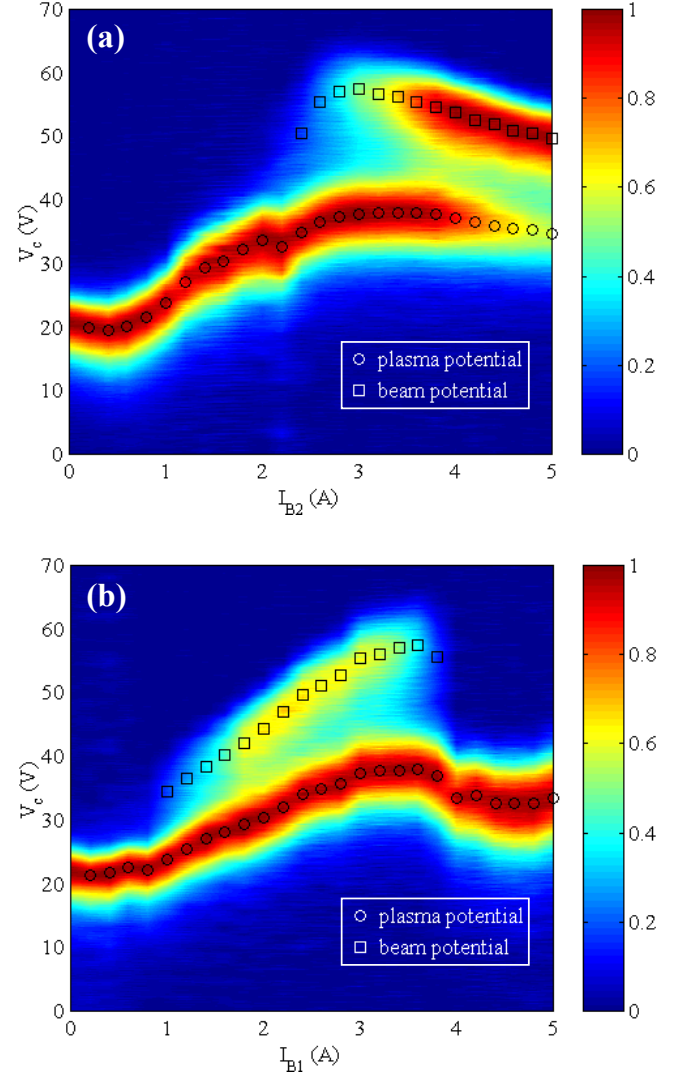


Fig. 6 (Color online) Contour plots of the normalized IEDFs (a) as a function of I_{B2} for $I_{B1} = 3$ A, and (b) as a function of I_{B1} for $I_{B2} = 3$ A, namely, the data are measured under the magnetic-field configurations presented in Figs. 5(a) and 5(b). The open squares and the open circles in Figs. 6(a) and 6(b) indicate the local plasma potential ϕ_p and the ion beam potential ϕ_{beam} , respectively.

Figure 6 shows the contour plots of the normalized IEDFs (a) as a function of I_{B2} for $I_{B1} = 3$ A, and (b) as a function of I_{B1} for $I_{B2} = 3$ A, namely, the data are measured under the magnetic-field configurations presented in Figs. 5(a) and 5(b). The open circles and the open squares shows the local plasma potential ϕ_p and the beam potential ϕ_{beam} estimated from the IEDFs. Considering the calculated magnetic-field configurations presented in Fig. 5, the conditions of $I_{B1} > I_{B2}$ and $I_{B1} < I_{B2}$ indicate the magnetic fields in the source tube is convergent and divergent, respectively. The former corresponds to $I_{B2} > 3$ A in Fig. 6(a) and $I_{B1} < 3$ A in Fig. 6(b), while the latter

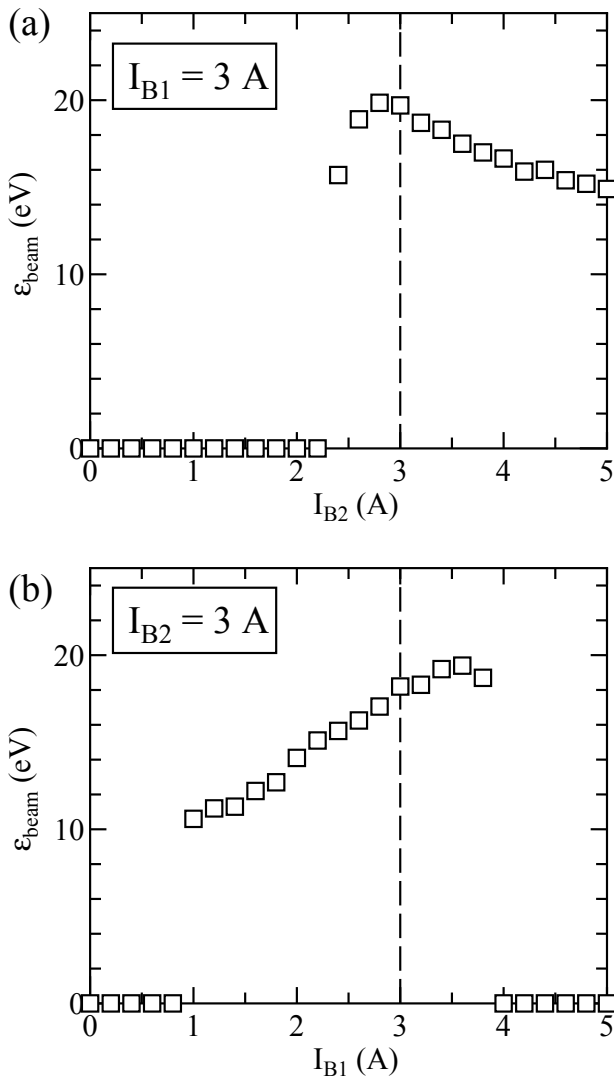


Fig. 7 Ion beam energy ε_{beam} (a) as a function of the exhaust-coil current I_{B2} for $I_{B1} = 3$ A, and (b) as a function of the upstream-coil current I_{B1} for $I_{B2} = 3$ A.

corresponds to $I_{B2} < 3$ A in Fig. 6(a) and $I_{B1} > 3$ A in Fig. 6(b). Figure 6(a) clearly shows that the ratio of the ion beam density to the bulk ion density increases with an increase in the exhaust-coil currents I_{B2} . In addition, the ion beam potential ϕ_{beam} has a maximum at $I_{B2} = 3$ A in Fig. 6(a) and at $I_{B1} = 3$ A in Fig. 6(b), respectively. That is to say, the beam potential shows the maximum when the magnetic-field strength inside the source tube is axially uniform. Under the magnetic-field configurations divergent inside the source tube, i.e., under the condition of $I_{B1} > I_{B2}$, it is found that the accelerated group ions are not detected at the downstream side of the source tube. In order to discuss the ion beam energy accelerated by the potential drop of the DL, the ion beam energy ε_{beam} ($\equiv \phi_{beam} - \phi_p$) should be estimated, since the local plasma potential ϕ_p is also changed for various

magnetic-field configurations.

From the data of the local plasma potentials and the beam potentials, plotted in Fig. 6 as open circles and open squares, the ion beam energy ε_{beam} is estimated. Figures 7(a) and 7(b) show the estimated ion beam energies ε_{beam} as a function of the exhaust-coil current I_{B2} for $I_{B1} = 3$ A, and as a function of the upstream-coil current I_{B1} for $I_{B2} = 3$ A, respectively. The dashed lines in Fig. 7 indicate the condition of $I_{B1} = I_{B2}$, i.e., the uniform magnetic-field configuration inside the source tube. The ion beam energy ε_{beam} is also found to have a maximum for the condition of $I_{B1} \simeq I_{B2}$. Therefore, we can deduce that the magnetic-field configuration with uniform fields inside the source tube and expanding fields near the source exit is effective for an increase in the energy of the supersonic ion beam.

4. Discussion

Here, we discuss the design of the PMs expanding plasma source. As described in our previous paper [15], the PMs expanding plasma source has double concentric arrays of the PMs with different diameter, which located at different axial positions. The specific configuration of the PMs can provide the constant magnetic fields inside the source tube and the divergent magnetic-fields near the source exit; then the rapid potential drop of a few tens volts and the supersonic ion beam are generated in the diffusion chamber. Based on the present results shown in Sec. 3, the previously reported configurations is guessed to be most effective for generation of the higher energy ion beam. This fact is required to be verified using the PMs expanding plasma machine in the near future, where the magnetic fields resembling the configuration shown in Fig. 5 can be produced by changing the axial position of the PMs array.

5. Conclusion

The effects of the magnetic-field configuration inside the source tube is experimentally investigated for the purpose of the optimization of the PMs expanding plasma source, where the new machine with the two solenoid coils for creating the divergent magnetic-field configuration is manufactured recently. The IEDFs near the source exit show the accelerated group of ions in addition to the bulk ions. The accelerated group of ions cannot be detected under the magnetic-field configurations diverging inside the source tube. The ratio of the ion beam density to the bulk ion density appears to increase for the magnetic-field configurations converging inside the source tube. It is demonstrated that the energy of the ion beam has a maximum when the magnetic-field strength in the source tube is ax-

ially uniform. The results would play an important role in the optimization of the recently-developed expanding plasma source using permanent magnets [15], which can generate the supersonic ion beam due to a formation of the DL.

Acknowledgements

The authors are indebted to H. Ishida and M. Sato for his assistance for constructing the solenoid coils. K. Takahashi and Y. Shida also thank to nice machines of mechanical working in the factory of the Dept. of E.E. Engineering, Iwate Univ., which are used for constructing the handmade machine presented here. This work is partially supported by a Grant-in-Aid for Young Scientists (B, 20740317) from the Ministry of Education, Culture, Sports, Science and Technology, Japan. This work is also partially supported by Yazaki Memorial Foundation for Science and Technology, and the Foundation for the Promotion of Ion Engineering.

- [1] C. Charles, *Plasma Sources Sci. Technol.* **16**, R1 (2007), and references therein.
- [2] C. Charles, *J. Phys. D: Appl. Phys.* **42**, 163001 (2009), and references therein.
- [3] R. E. Ergun, Y. -J. Su, L. Andersson, C. W. Carlson, J. P. MacFadden, F. S. Mozer, D. L. Newman, M. V. Goldman, and R. J. Strangeway, *Phys. Rev. Lett.* **87**, 045003 (2001).
- [4] R. W. Boswell, E. Marsch, and C. Charles, *Astrophys. J.* **640**, L199 (2006).
- [5] N. Plihon, P. Chabert, and C. S. Corr, *Phys. Plasmas* **14**, 013506 (2007).
- [6] K. Takahashi and T. Fujiwara, *Appl. Phys. Lett.* **94**, 061502 (2009).
- [7] S. A. Cohen, N. S. Siefert, S. Stange, R. F. Boivin, E. E. Scime, and F. M. Levinton, *Phys. Plasmas* **10**, 2593 (2003).
- [8] X. Sun, A. M. Keesee, C. Biloiu, E. E. Scime, A. Meige, C. Charles, and R. W. Boswell, *Phys. Rev. Lett.* **95**, 025004 (2005).
- [9] S. C. Thakur, Z. Harvey, I. A. Biloiu, A. Hansen, R. A. Hardin, W. S. Przybysz, and E. E. Scime, *Phys. Rev. Lett.* **102**, 035004 (2009).
- [10] K. Takahashi, C. Charles, R. W. Boswell, T. Kaneko, and R. Hatakeyama, *Phys. Plasmas* **14**, 114503 (2007).
- [11] K. Takahashi, C. Charles, R. W. Boswell, and R. Hatakeyama, *Phys. Plasmas* **15**, 074505 (2008).
- [12] K. Takahashi, C. Charles, R. W. Boswell, W. Cox, and R. Hatakeyama, *Appl. Phys. Lett.* **94**, 191503 (2009).
- [13] A. Meige and R. W. Boswell, *Phys. Plasmas* **13**, 092104 (2006).
- [14] M. D. West, C. Charles, and R. W. Boswell, *J. Popul. Power* **24**, 134 (2008).
- [15] K. Takahashi, K. Oguni, H. Yamada, and T. Fujiwara, *Phys. Plasmas* **15**, 084501 (2008).
- [16] K. Takahashi, Y. Shida, T. Fujiwara, and K. Oguni, *IEEE Trans. Plasma Sci.* **37**, 1532 (2009).
- [17] K. Takahashi, Y. Shida, and T. Fujiwara, submitted to *Plasma Sources Sci. Technol.*.
- [18] C. Charles, *Phys. Plasmas* **12**, 044508 (2005).
- [19] C. Charles, *IEEE Trans. Plasma Sci.* **36**, 2141 (2008).
- [20] K. Takahashi, T. Kaneko, and R. Hatakeyama, *Plasma Sources Sci. Technol.* **15**, 495 (2006).
- [21] K. F. Schoenberg, *Rev. Sci. Instrum.* **49**, 1377 (1978).
- [22] K. Takahashi and T. Fujiwara, to be published in JAXA Research and Development Report (2009).
- [23] C. Charles and R. W. Boswell, *Phys. Plasmas* **11**, 1706 (2004).